

This discussion paper is/has been under review for the journal Hydrology and Earth System Sciences (HESS). Please refer to the corresponding final paper in HESS if available.

Identification of glacial melt water runoff in a karstic environment and its implication for present and future water availability

D. Finger^{1,2,*}, A. Hugentobler^{1,2}, M. Huss³, A. Voinesco^{3,4}, H. Wernli^{1,2},
D. Fischer^{1,2}, E. Weber⁵, P.-Y. Jeannin⁵, M. Kauzlaric^{1,2}, A. Wirz^{1,2},
T. Vennemann⁶, F. Hüsler^{1,2}, B. Schädler^{1,2}, and R. Weingartner^{1,2}

¹Institute of Geography, University of Bern, Bern, Switzerland

²Oeschger Centre for Climate Change Research, University of Bern, Bern, Switzerland

³Department of Geosciences, University of Fribourg, Fribourg, Switzerland

⁴Institute of Geography, University of Neuchâtel, Neuchâtel, Switzerland

⁵Swiss Institute of Speleology and Karst-Research, La Chaux-de-Fonds, Switzerland

⁶Institute of Earth Sciences, University of Lausanne, Lausanne, Switzerland

*now at: Department of Geography, University of Zurich, Zurich, Switzerland

2743

Received: 11 January 2013 – Accepted: 14 February 2013 – Published: 6 March 2013

Correspondence to: D. Finger (fingerd@gmx.net)

Published by Copernicus Publications on behalf of the European Geosciences Union.

Abstract

Glaciers all over the world are expected to continue to retreat due to the global warming throughout the 21st century. Consequently, future seasonal water availability might become scarce once glacier areas have declined below a certain threshold affecting future water management strategies. Particular attention should be paid to glaciers located in a karstic environment, as parts of the melt water can be drained by souterrain karst systems. In this study tracer experiments, karst modeling and glacier melt modeling are combined in order to identify flow paths in a high alpine, glacierized, karstic environment (Glacier de la Plaine Morte, Switzerland) and to investigate current and predict future downstream water availability. Flow paths through the karst underground were determined with natural and fluorescent tracers. Subsequently, tracer results and geologic information were assembled in a karst model. Finally, glacier melt projections driven with a climate scenario were performed to discuss future water availability in the area surrounding the glacier. The results suggest that during late summer glacier melt water is rapidly drained through well-developed channels at the glacier bottom to the north of the glacier, while during low flow season melt water enters into the karst and is drained to the south. Climate change projections reveal that by the end of the century glacier melt will be significantly reduced in the summer, jeopardizing water availability in glacier-fed karst springs.

1 Introduction

Global warming has led to a drastic reduction of glacier volume in many mountain regions of the world (Dyrgerov and Meier, 2000; Kaser et al., 2006). This reduction will subsequently affect glacier melt runoff, affecting downstream water resources (Farinotti et al., 2012). In alpine regions this will affect valuable water usages such as hydropower production (Finger et al., 2012; SGHL, 2011), agriculture, tourism, and snow production (FOEN, 2012; Reynard, 2000). Predictions are complex, as melt water drainage from

2745

the glaciers is subject to diurnal variability (Schuler et al., 2004) and may evolve during the melting season due to enhanced melting (Covington et al., 2012) and glacial lake outbursts (Werder et al., 2009). In karstic environments such projections become even more difficult as runoff paths are underground and therefore difficult to observe and assess (Bonacci et al., 2006; Siemers and Dreybrodt, 1998). In many situations the proportion of water from a glacier to a karst spring are unknown and conversely, the number of springs fed by a glacier are difficult to estimate (Gremaud and Goldscheider, 2010; Gremaud et al., 2009; Jobard and Dzikowski, 2006).

In recent years investigations of the interaction of glacier-groundwater below the Pleistocene ice shields have been performed (Flowers et al., 2003) and the cooling of the alpine massif due to melt water infiltration has been investigated (Marechal et al., 1999). However, few studies have assessed the relation between alpine glaciers and connected aquifers (Smart, 1996). Nevertheless, in the European Alps many communities and ecosystems depend on water resources originating either directly from the glacier melt or from karst springs fed with glacier melt water. However, it is essential for water managers to understand the origin of water resources in order to adapt adequate water management strategies to cope with the impacts of climate change on water resources (FOEN, 2012). A drastic decrease in glacier volume can lead to a desiccation of karst springs fed by water from glaciers. In remote mountain areas this could lead to water shortages, as replacement water would have to be transported from far away to regions lacking glacial melt water.

Recent research has been focusing on assessing water resources from karstic environment using karst models (Butscher and Huggenberger, 2009; Doerfliger et al., 1999; Jeannin et al., 2012a), artificial tracer experiments (Goldscheider et al., 2008) and chemical and isotopic composition in runoff water (Grasso and Jeannin, 2002). To assess current and future water resources, it is necessary to combine the three techniques and combine the results in one illustrative karst model. The integrative assessment of karst modeling, natural and artificial tracer experiments and climate change projections of glacier retreat allows assessing future water resources.

2746

A typical example of a karstic environment in the Alpine region is the Glacier de la Plaine Morte (PM) in the Bernese Oberland, Switzerland (Maire, 1977; Wildberger, 1979). The present study presents a combination of natural and fluorescent tracer investigations, karst modeling and glacier melt modeling to identify current and future pathways of glacier melt water through the karst to downstream areas of interest. For this purpose a 3-D karst model was established using topographic and geological information in order to design tracer experiments that allow determining the melt pathways. Subsequent to tracer injection on the glacier tracer concentrations, discharge and meteorological parameters were measured at all relevant locations. Subsequently, the karst model was validated and revised with the results of the tracer experiments. In order to assess future water availability, climate change projections of glacial melt water were performed using a dynamic glacier model. The study concludes by discussing probable trends in water resources at designated karst springs around Glacier de la Plaine Morte. Although the specific results are only valid for the presented case study, the proceeding and the general conclusions discussed in the paper can apply to any karstic mountain area.

2 Study site

The glacier de la Plaine Morte in the Bernese Oberland was selected for this study, as it represents a typical example of an alpine karstic environment, where downstream ecosystems and economic uses depend on glacial and rainfall runoff. The main characteristics of the study site are summarized below.

2.1 Glacier de la Plaine Morte

The Glacier de la Plaine Morte is a large plateau glacier that is situated in southern Switzerland on the main water divide between the Rhine and Rhone at the border of the cantons Bern and Valais (Fig. 1a and b). The glacier is characterized by an almost

2747

5 km wide plateau at an altitude ranging between 2700 and 2800 m a.s.l., and a small and narrow glacier tongue, also called Retzligletscher, descending in northern direction (Fig. 1c). Since 1985 the glacier was completely snow-free during most summers due to its low elevation. A snow free glacier features lower surface albedo and thus enhances the effects of direct solar radiation on glacier melt (Bühlmann, 2011; Paul et al., 2005). In 2011, the glacier covered a total area of approximately 8 km² and reaches thicknesses of more than 200 m (Voinesco, 2012). The total ice volume of the Plaine Morte is 0.76 km³ (in 2011) which corresponds to 1–1.5 % of the total glacier ice volume in the Swiss Alps (Farinotti et al., 2009).

The skiing resort Crans-Montana (CM) is situated south of the glacier. Water requirements in Crans-Montana peak during summer due to irrigation demands and in winter due to snowmaking demands (Reynard and Bonriposi, 2012). In the North of the glacier, agricultural areas in the Simmen valley depend on precipitation and melt water from the Plaine Morte region. In the Simmen valley water demands are similar to the Crans-Montana region, as water is being pumped from the River Simme to surrounding skiing resorts for snow production in winter and for irrigation to agricultural areas in the valley bottom in the summer. Consequently, a reduction of water availability might intensify and sharpen the political discussions about water uses for irrigational purposes, snow production, hydropower production and drinking water (Reynard and Bonriposi, 2012).

2.2 Geologic setting

Being part of the Helvetic Nappes, the geology surrounding the Plaine Morte is mainly composed of limestone (Fig. 2). As is the case for most nappes, the limestones are aligned in parallel to the topography, i.e. striking the south-east flank of the Crans-Montana region, sub horizontal below the Glacier de la Plaine Morte and steep towards north-west. In the front of the nappes a reversed dip can be expected. In the investigated area three main nappes lying on top of the Eastern end of the Aare massive have been identified (Badoux, 1945; Gabus et al., 2008; Wildberger, 1979). The Doldenhorn

2748

Nappe is the lowest one with a thick series of limestone separated by some shaly layers. The Gellihorn Nappe is much thinner and of limited significance for the present work. The Wildhorn Nappe is the most relevant one for the present study because most of the outcropping rocks belong to this upper unit. It encloses two main karstified layers forming two karst aquifers: the Urgonian limestone and the Malm limestone (Fig. 2). The upper limestone drains most of the infiltration waters. Marls and shales represent more or less impermeable barriers between the two main karst aquifers.

The karstic area drains most of the precipitation and melt-waters and a series of karst springs have been identified all around the area, on both sides of the water divide (Wildberger, 1979). The catchment areas of the respective springs are not well delineated, making it difficult to assess water availability on each side.

2.3 Hydrology

Discharge from snow and ice melt, as well as rainfall runoff is characterized by six mechanisms of the land use characteristics in the Plaine Morte area: (i) water retentions in the glacier and the snow fields, (ii) rapid subsurface flow under gravel covered soil, (iii) low flow in fertile agricultural soil, (iv) retention in natural swamps, (v) storage in natural and artificial lakes and (vi) a well-developed karst system which drains melt water to karstic springs at lower elevations.

In the upper part above 1500 m a.s.l. the stream network is poorly developed, showing a high proportion of screes and karsts (Maire, 1978). This region corresponds to the water divide between Rhone and Rhine rivers, and also between two cantons Bern and Valais (Fig. 1b). The Glacier de la Plaine Morte represents a huge water reservoir which has been continuously declining due to warmer temperatures during recent decades. The detailed mapping of mountain creeks in this area is impossible as water flow paths are on the surface as well as in the karst. Karst water is drained to numerous karst springs surrounding the glacier at lower elevation, such as the Siebenbrunnen (SB) spring in the north and the Loquesse (L) spring in the south west (Fig. 1c). Accordingly,

2749

discharge is highly variable and depends on the property of the upstream soil and land use properties.

Surface torrents and rivers mostly occur below 1500 m asl with numerous mountain creeks, all emerging from karst springs. The Tièche river, coming from the south-eastern part of the Plaine Morte, and the Trübbach, emerging from the northern end of the Plaine Morte are exceptions. The two rivers are primarily fed with glacier melt water and several small karst springs emerging along the flow line. The Trübbach enters a few hundred meters downstream of the Siebenbrunnen spring into the Simme river which drains the water to the north, passing the village of Oberried (OR) and Grubenwald (GW), both sampling location during the tracer experiments.

The permeable nature of the karst massif explains the restricted number of lakes in this periglacial landscape. The main exception is the Lac de Tseuzier (LT), which is an artificial hydropower reservoir operated by the *Lienne SA* hydropower company. The other lakes are small and mostly temporary.

On the southern side of the Plaine Morte the natural drainage patterns are additionally influenced by channels following almost horizontally along the flanks of the mountains to divert water for irrigational purposes (Crook and Jones, 1999).

3 Methods and data

In order to identify and analyze the flow paths of glacier melt water in the Plaine Morte area and discuss possible effects of climate change on water resources, a variety of measurements and modeling tasks were performed. In a first step all geologic and hydrologic information was assembled in a karst model in order to set up an adequate strategy for natural and artificial tracer investigations. Subsequently, artificial tracer experiments, as well as isotopic natural tracer measurements in the runoff were performed in order to assess the primary pathways of melt water. Furthermore, snow cover data derived from satellite imagery and meteorological data from three weather stations were available for the entire investigation period. Complementary, gauging stations

2750

were installed at relevant locations during the tracer experiments. Finally, the future melt water generation was estimated with a glacier melt and retreat model driven with climate scenarios forced with A1B emission scenarios. All datasets available for this study are summarized in Table 1 and details of data collections are described below.

5 3.1 Karst model

All existing geological information (Sect. 2.2 and Table 1) were assembled into a 3-D geological model using the software package CINEMA 4D (MAXON Computer GmbH). During this process local inconsistencies from the different geologic maps were corrected. For this purpose information from existing literature was considered in order to incorporate a maximum of available information. This model was built according to the “KARSYS approach” (Jeannin et al., 2012b), which is being developed within the framework of the *Swisskarst* project (<http://www.swisskarst.ch>), part of the NRP 61 program.

For the construction of the geological model three data sources were used: (i) four geological maps at a scale of 1 : 25 000 (Swisstopo); (ii) 15 geological cross sections and (iii) a DEM with 25 m gridding (Swisstopo).

Once the geometry of the main aquifer (Urgonian limestone) was defined, the main springs discharging water from this aquifer were introduced into the 3-D model. Due to high hydraulic conductivity of karst conduits, it can be assumed that the hydraulic gradient upstream from the springs is lower than 1 %. Therefore, the volume of aquifer located below the level of the springs can be considered as the phreatic part of the karst aquifer. During high water conditions the top of the phreatic zone may rise up by dozen, or even hundreds of meters (Wildberger et al., 2001).

In Fig. 3 an illustration of the assembled information of the karst model is given. The structure of the karst model plunges towards the west and is not cylindrical. The landscape cuts this structure according to the mountainous relief of this region, and the intersection between topography and geology is therefore quite complex.

2751

The 3-D karst model is an ideal tool to understand karst flow-paths in such a complex setting and develop hypothesis for successful tracer experiment set ups, as illustrated in Fig. 3 with three tracer injection points on the glacier. It allows to build the geometry of the main aquifers in 3-D and to apply some basic principles of karst hydraulics (KARSYS approach). The final model obtained using also the results from the tracer experiments is presented in the result section of this study.

3.2 Monitoring of meteorological and snow cover conditions

Meteorological conditions during the tracer experiments were available from three weather stations located at W1, W2 and CM (Fig. 1) operated by the *Institute for Snow and Avalanche Research* (SLF), by the *Remontée mécaniques de Crans-Montana* (CMA) and the *Federal Office of Meteorology and Climatology* (MeteoSwiss), respectively. The ratio of snow cover area with the watershed of the Simme and the Liène (Fig. 1) was derived from daily satellite images recorded by the moderate resolution imaging spectroradiometer (MODIS) (Hall et al., 2002). Similarly to Hüsler (2012) and Finger et al. (2011) the MODIS product MOD10A1.5 (see <http://nsidc.org/>) was used in this study. Total discharge into Lac de Tseuzier computed from water release and lake level recordings were provided by *Lienne SA*, discharge at GW and OR were made available by the *Swiss Federal Office of Environment* (FOEN). At TB, SB and L continuous discharge was estimated with pressure sensors converted to continuous discharge time series based on periodic discharge measurements using the salt method as described in Hugentobler (2013).

3.3 Tracer experiments

In order to identify flow path ways of melt water from the Plaine Morte five tracer experiments were conducted using three different fluorescent tracers (Table 2). The objective of these experiments was to assess the spatial contribution of melt water from different

2752

glacier regions as well as the seasonal evolution of melt drainage due to changing hydro-meteorological conditions.

The first three experiments were carried out simultaneously on 22 August 2011 in order to assess the contribution of ice melt from three representative regions of the glacier to runoff. According to the geologic information assembled in the karst model (Sect. 3.1; Fig. 3) the glacier can be divided into three regions: (i) north-western region which is expected to drain via the large syncline towards the Loquesse spring. However, the presence of faults cutting the north-western anticline makes it also possible for water to flow also towards the north-west, to Bernese karst springs. (ii) The central region is expected to drain towards the Loquesse spring through the southern, narrower syncline. A connection to Bernese springs is not probable unless shallow holes along the Trübbach make such a connection possible. (iii) The southern region which is expected to drain through a path along the southern syncline to the Loquesse spring. Previous tracer experiment by Crestin (2001) indicate drainage from this region towards the south.

To validate these assumptions 36 kg eosine, 38.8 kg duasyne and 12 kg uranine were added to the melt water at three locations (I1, I2 and I3) on the glacier. The objective of performing three simultaneous tracer experiments was to investigate melt pathways from the northern region of the glacier (represented by I1), the southern region of the glacier (represented by I2) and the eastern region of the glacier (represented by I3). Accordingly, eosine was injected at a northern location (I1), duasyne at a south western location (I2) and uranine at a south eastern location on the glacier (Fig. 1 and Table 2). In the following three months water samples were collected at 30 karst springs and surface runoff around the Plaine Morte area. Samples were collected at 10 locations with automatic samplers and 20 further locations manually. During the first 42 h after tracer injections, automatic sampling was conducted with hourly resolution and manual sampling was conducted with 6 h resolution. In the following seven days automatic sampling frequency was reduced to 4 h intervals, while manual sampling was performed every eight hours. Subsequently, the following 11 days automatic sampling

2753

was reduced to 6 h intervals, while manual sampling was reduced to daily samples. Sampling at all automatic sampling location was continued for two months with daily frequency to monitor retarded tracer amounts.

On 6 August 2012 and 2 September 2012 two supplementary tracer experiments were carried out by injecting uranine about 600 m south of location I2. The objective of these experiments was to investigate the evolution of melt pathways in the glacier before and after intense melting periods.

Tracer concentrations in collected water samples were determined in the lab by initiating the tracer in a LS-5B Perkin-Elmer luminescence spectrometer. Uranine was illuminated at 490 nm, eosine at 512 nm and duasyne at 449 nm. Respectively, emissions from the three tracers were measured at 515, 537 and 474 nm. Tracer concentration is directly proportional to the fluorescence emission of the tracer.

3.4 Isotope measurements

In order to investigate the provenance of runoff water in karst springs, measurements of isotopic compositions were made on water samples from the test site. For this purpose water samples were collected during the entire melting phase (from June to September) from karst springs on the south slope of the Plaine Morte (Loquesse, Ertëntse and Tièche; Fig. 1), from melt water of snow fields and from rain gauges in which local precipitation was collected. The H- and O-isotope composition was measured using a Wavelength-Scanned Cavity Ring Down Spectroscopy (WS-CRDS) system (Picarro L1102i). The instrument was calibrated before every measurement sequence using three internal standards and normalized on the international scale of VSMOW and SLAP (Coplen, 1994). The uncertainty of the technique lies at $\pm 0.07\%$ for O- and $\pm 0.4\%$ for H-isotope compositions given on the familiar δ -scale in parts per thousand relative to VSMOW.

2754

3.5 Glacier melt modeling

Melt water runoff and glacier evolution of the Glacier de la Plaine Morte is calculated using the glacio-hydrological model GERM (Huss et al., 2008). The model accounts for the spatial distribution of snow accumulation, snow- and ice melting, glacier geometry change, evaporation and runoff routing. The amount of melting is simulated based on an enhanced temperature-index model (Hock, 1999) accounting for temporal and spatial variations in potential solar radiation. Glacier geometry change is calculated using a simple parameterization of glacier retreat and measured ice thickness distribution (Huss et al., 2010). The model is run on a 25 × 25 m grid at daily resolution and provides runoff components from the entire basin of the Plaine Morte, as well as annually updated ice-covered areas and glacier ice volumes.

The model is driven using daily mean air temperature and precipitation recorded at an automatic weather station maintained by MeteoSwiss at Crans-Montana and is calibrated using the observed ice volume change of the Plaine Morte. Volume change for the period 1956–2005 is obtained by the differencing of two digital elevation models that are based on a topographical map, and aerial photogrammetry (Bauder et al., 2007). Model results are validated against direct observations of winter snow accumulation at up to 100 measurement sites, and summer ablation at 4 locations on the glacier surface for the hydrological years 2010 to 2012.

In order to provide perspectives on future hydrological impacts of the ongoing glacier retreat, model runs were performed for the period 2010–2100 using climate scenarios forced with the A1B emission scenario. The glacio-hydrological model was forced using probabilistic changes in seasonal air temperature and precipitation based on the median of 10 Regional Climate Models for the alpine region (Frei, 2007; Huss et al., 2010).

2755

4 Results

4.1 Meteorological and hydrological observations

The meteo-snow and hydrological conditions before, during and after the tracer experiments are of major relevance for interpreting the tracer experiment results, as discussed in the discussion section. The dynamics of snow cover depletion and melt water pathways strongly depend on local air temperature and precipitation. As the glacier is temperate (i.e. at the pressure-melting point) throughout the entire ice volume plastic deformation of ice is an important process leading to a relatively rapid closure of empty glacial voids and drainage channels when the water input into the system is reduced, i.e. the channels are no longer supported by water pressure (Röthlisberger, 1972). On Glacier de la Plaine Morte, this was directly observed in bore holes (M. Schwikowski, personal communication, 2012).

The evolution of daily mean air temperature and snow height at locations W1, W2 and CM (Fig. 1), average daily discharge into Lac de Tseuzier and in Oberried are illustrated in Fig. 4. Mean air temperature between January and September in 2011 and 2012 in CM were 8.5 and 7.4 °C, respectively (Fig. 4a). Concurrently, mean snow heights at M1 were 88 cm in 2011 and 127 cm in 2012. This falls in line with the ratio of snow cover area (SCA) in the watershed derived from satellite images. In 2011 SCA dropped below 50 % end of March, while SCA in 2012 remained above 50 % until end of April (Fig. 4b). Due to the intense snow falls in 2012, mean discharge between January and September into Lac de Tseuzier and at Oberried increased in 2012 by about 30 % at both locations compared to 2011 (Fig. 4c).

In regard to the interpretation of the tracer experiment results, particular attention should be given to the meteorological conditions just before the tracer experiment. Just before the three simultaneous tracer injections in 2011 (S2 in Fig. 4), air temperature on the Plaine Morte was well above freezing point and the glacier had been snow free for several weeks. This would represent a condition with intense glacier melt and well developed melt path ways in the glacier. The date of the tracer experiment performed

2756

on 6 August 2012 (S1 in Fig. 4) was the first day when the glacier became completely snow free and an injection was possible. Nevertheless, it was also preceded by a warm period with enhanced snow melt. The last tracer experiment performed on 2 September 2012 (S3 in Fig. 4) was supposed to represent the conditions at the end of the melting season with very well developed melt canals in the glacier. However, two days before the injection a cold front arrived, temperatures dropped below freezing and heavy snow fall covered the entire glacier with about 40 cm fresh snow.

4.2 Tracer experiment results

In the following we first present the results of the three simultaneously performed tracer experiments in August 2011 and then the two complementary tracer experiments performed in August and September 2012 (Table 2).

The objective of the three simultaneously performed tracer experiments with three different tracers injected at three different locations (Fig. 1c) distributed on the glacier was to determine melt pathways from the three regions of the glacier (Sect. 3.3). The observed evolution of the three tracer concentrations is illustrated in Fig. 5. The only locations out of the 30 sampling locations where tracers were detected were the Loquesse spring (location L) in the southwest, the Siebenbrunnen spring in the north (SB), the Retzliberg spring (R) and in Trübbach (TB) and Simme (OR and GW). As shown in Fig. 5, the highest tracer concentrations were detected in the River Simme at OR and GW only a few hours after tracer injections. Indeed, a large amount of glacier runoff drained from the area via the Trübbach, the surface runoff entering into the river Simme. Maximum tracer concentrations were reached a few hours after injections reaching over 850 mg m^{-3} of eosine, 200 mg m^{-3} of uranine and 220 mg m^{-3} of duasyne. The exact temporal delay between injection and tracer detection at TB is unknown, as sampling frequency in 2011 was too low. Very high concentrations of duasyne were also recorded at the Loquesse spring, reaching over 200 mg m^{-3} 25 h after injection. Small amounts of uranine and eosine were also recorded at the Siebenbrunnen spring 26 h after tracer injection. Duasyne was also detected at Siebenbrunnen,

2757

but with a delay of 47 h after injection. Maximum tracer concentrations recorded at Siebenbrunnen were 3.4 mg m^{-3} of eosine, about 1 mg m^{-3} of uranine and less than 0.5 mg m^{-3} of duasyne. In the small Retzliberg spring similar concentrations were found, however, first arrival of tracers was almost 12 h before detection at Siebenbrunnen.

By integrating the product of observed tracer concentration and recorded discharge the amount of tracer passing at the different locations can be quantified. All estimated loads are summarized in Table 3. The load estimates indicate that in Grubenwald about 22 % of the injected duasyne, 82 % of the uranine and the entire amount of eosine were transported into the Simme River during the first 3 days after tracer injection. Very small loads were registered at the karst springs on the Bernese side at Siebenbrunnen and Retzliberg. About 24 % of the injected duasyne was detected on the Valais side in the Loquesse spring. No tracers were found at all other locations. The tracer loads listed in Table 3 have to be interpreted with caution as load estimates are subject to uncertainties due to low sampling frequency, tracer degradation and uncertainty in discharge estimations.

The arrival time of the first tracer at each location indicates the flow velocity of melt water relative to the injection point on the glacier and over the surface to the sampling locations (Table 3). At all karst springs (L, SB and R) the flow velocity was less than 0.4 km h^{-1} , falling in line with observations from previous tracer experiments (Wildberger, 1979). Mean flow velocities computed from the time delay between injection and tracer registrations at locations in surface waters indicate velocities of more than 2 km h^{-1} .

The objective of the two complementary tracer experiments performed in August and September 2012 was to demonstrate how melt paths and glacier discharge patterns evolve over the course of one melting season. The experiments were only performed with uranine, every time injected close to the south western location (I2). The injection in 2012 was about 600 m west of the injection in 2011, which might also have had an impact on the results.

Together with the duasyne-tracer injection in August 2011 tracer evolution in downstream waters could be assessed for three different situations (S) covering the evolution of melt pathways during an entire melting season: (S1) the injection on 2 August 2012 represents the very start of the ice melting season, as it was performed on the first day the glacier became snow free and an injection became possible, (S2) the injection on 22 August 2011 represents the period of maximal ice melting as it was preceded by a intense melting period and (S3) the injection on 6 September 2012 reveals melt pathways after a cold front covered the region with snow. The concentrations recorded in downstream karst springs during the three experiments are illustrated in Fig. 6. The temporal evolution of tracer concentration recorded in the surface runoff on the northern side of the glacier (Location GW) indicates that travel time between S1 and S2 is similar. In both situations the tracer was recorded in GW 8.5 h after the injection. This is reasonable, as both S1 and S2 were preceded by intense melting and pathways in the glacier leading to the northern surface creek could already be well developed and water pressure was high enough to enable water runoff over the northern surface torrent. The evolution of the concentration also reveals that the tracer reached TB and OR after about 4.5 h, confirming the high flow velocities of almost 4 km h^{-1} observed in the 2011 experiment (Table 4). During the tracer experiment in September 2012 no tracer could be detected on the Bernese side of the glacier, indicating that water content in the glacier was reduced and subsequently melt water was trapped in the depressions of the glacier basin, as outlined in the discussion section.

The evolution of tracer concentration detected in the karst spring SB is illustrated in Fig. 6b. In S1 (experiment in August 2012) tracer was already recorded 24 h after injection, revealing a maximal flow velocity of 0.2 km h^{-1} (Table 4). In S2 in August 2011 the tracer was only detected at SB 46 h after injection. Accordingly, the computed flow velocity in S1 is almost twice the flow velocity observed during S2, indicating lower water pressure reducing the karst through flow. To some extend the slightly different injection location may also have influenced the flow velocity.

2759

Finally, tracer concentrations detected at the karst spring L on the southern side of the glacier are illustrated in Fig. 6c. Tracer was detected at L during all three tracer experiment, making it the only location where the effects of meteo- and hydrological conditions on glacier melt runoff through the karst can be observed. In August 2012 (S1) the tracer was detected 14.75 h after the injection, in August 2011 (S2) the tracer took 19 h to reach L and in September 2012 (S3) the tracer arrived 40 h after injection. Accordingly, flow velocities were reduced from 0.5 km h^{-1} (S1), to 0.3 km h^{-1} (S2) and finally to 0.2 km h^{-1} during the melt season (Table 4). This result falls in line with the decrease in flow velocities observed at SB between the injection in August 2012 (S1) and August 2011 (S2). These results support the assumption that with increasing melt water input, the flow paths in continuous channels in the glacier tend to dominate the karstic system and a higher percentage of runoff flows directly to the surface runoff on the northern side of the glacier. During S1 water reaches the bottom of the glacier, is trapped in the depressions of the glacier basin and primarily percolates into the karst system, while in S2 melt water is evacuated through the glacier to the surface runoff in the north. Furthermore, the experiment in September 2012 demonstrated that after an onset of winter conditions (S3) the flow paths to the north of the glacier are drastically reduced to local melt water runoff and melt water from the glacial potholes penetrates entirely into the karst.

4.3 Karst model results

The results of the tracer experiments were integrated into the 3-D karst model in order to visualize the flow paths of snow and ice melt water (Fig. 7). The final model demonstrates that most of the water infiltrating the ground in the southern part of the glacier is drained towards the Loquesse spring. However, the northern anticline is traversed by many faults and the geometrical interpretations of the synforms are not the same. The top of the aquiclude is probably not much higher than the groundwater and possibly at the same level at high water conditions in the Eastern part. An overflow towards the north (Siebenbrunnen) is therefore possible.

2760

The nature of the karst terrains around the glacier explains why the surface runoff network is poorly developed. The glacier itself lies on karstified limestone which is probably covered by impermeable lenses of fine sediment of glacial silk. Only in some areas the fine sediment is permeable, allowing water to infiltrate into the karst. This falls in line with observations of Wildberger (1979) who noted that about 50 % of glacier melt-water infiltrates into the karst while the rest is drained at the glacier mouth during high water conditions.

Wildberger (1979) also mentioned the presence of shallow holes in the stream bed of the Trübbach allowing part of the discharge to be infiltrated into the karst system shortly downstream of the glacier. This water is expected to reach karst springs on the Northern (Bernese) flank, i.e. Siebenbrunnen.

4.4 Isotopic compositions

In Fig. 8 the temporal evolution of the isotopic composition measured in karst springs on the southern slopes of the Plaine Morte massif is illustrated. Although the Tièche is sometimes fed with glacier water over the surface runoff, this was not the case during 2011. The striped area in the figure illustrates the range of the isotopic compositions reported from cores taken from the glacier by Schotterer et al. (2004). Results of snow samples collected in spring 2011 indicate that the snowmelt has an isotopic composition that is lower than -14.5‰ in $\delta^{18}\text{O}$ while the isotopic composition measured for precipitation in autumn of 2011 had values higher than -9‰ in $\delta^{18}\text{O}$. The temporal evolution of the isotopic composition in the karst springs south of the Plaine Morte indicates that in spring (May to June) and early July the isotopic composition is compatible with a high contribution of snow melt water. In all three springs the isotopic composition becomes enriched in the heavier isotopes in July, with an isotopic composition similar to that of the glacier as measured by Schotterer et al. (2004). In September the isotopic composition became even more enriched in the heavy isotopes, reaching similar values as measured in typical summer precipitation from the area. This suggests that

2761

while the karst springs may have been dominated by glacial melt waters in August, runoff might be dominated in September by local rainfall runoff.

4.5 Present and future runoff from Glacier de la Plaine Morte

Modeling of melt water runoff throughout the summer season 2011 shows that during warm late-summer days more than $7\text{ m}^3\text{ s}^{-1}$ of discharge can be generated by ice melting only (Fig. 9). This number refers to a daily mean; as glacial runoff shows strong diurnal variations (Jansson et al., 2003) and maximal runoff in the afternoon can be significantly above $10\text{ m}^3\text{ s}^{-1}$. The tracer experiments in August 2011 took place during a phase of strong glacier melt. One week of high melt-water input into the glacial drainage system preceded the tracer experiment which took place close to the overall maximum runoff in the year 2011.

Due to the comparably thick ice and the limited surface slopes, the Plaine Morte is expected to show an atypical retreat behavior. Future glacier change is mainly characterized by a strong lowering of the entire glacier surface, but only a limited loss in glacier area over the next decades (Fig. 10). This leads to progressively more negative glacier mass balances due to several positive feedback effects. The climate projections indicate that by 2080 the Plaine Morte will be reduced to a few isolated ice patches. The dynamic of glacier retreat has a significant impact on the runoff from the catchment that is currently occupied by the Plaine Morte. Whereas runoff is expected to increase initially, peaking between 2040 and 2060, due to the release of water from glacial storage, overall basin discharge will decrease below the current level by the end of the century, and it is then dominated primarily by precipitation. The changes in summer runoff are even more important. Whereas runoff is concentrated in July and August at present (almost 60 % of annual runoff), summer runoff from the basin of the Plaine Morte will drastically decrease until 2100 and drop to less than 20 % of the amount found for the first half of the 21st century.

2762

5 Discussions

5.1 Validation of the karst model

Results of the tracer experiments reflect well the hypothesis on flow paths formulated before the experiment with the karst model. The three simultaneous tracer experiments in 2011 clearly indicate that glacial melt water from all regions of the glacier is transferred through the glacier to the surface runoff into the Simme valley on the northern side of the glacier. This surface runoff is very rapid and reaches mean velocities of up to 3 km h^{-1} . The main surprise is the amount and the speed of water transferred directly below the glacier towards the Trübbach. The fact that all three tracers were detected within a few hours at the glacier mouth and this without any precipitation occurring over this interval implies that during intense melting, melt water follows primarily continuous channels through the glacier to the lowest surface runoff Trübbach on the northern side of the glacier. As the bottom topography of the glacier measured by geophysical investigations indicated three depressions (Fig. 10), This can only be the case if the water table within the glacier is high enough to overcome the depression of the glacier basin (Fig. 11a). These findings have to be considered in regard to the extreme weather conditions of 2011. Recordings at the weather station at CM reveal that air temperature were 2.1°C warmer and 12 more summer days (max temperature exceeding 25°C) were recorded in 2011 than long-term averages. Indeed, the warm temperatures connected with below-average winter accumulation led to strongly negative glacier mass balances of $-2.13 \text{ mweq yr}^{-1}$ in 2011 (Voinesco, 2012). In addition, the formation of several ice marginal lakes with a volume of several $100\,000 \text{ m}^3$ was observed (Fig. 1). These lakes drained within hours about one month before the tracer experiment (Hählen, 2012). It can be assumed that the sudden water input of glacier-dammed lakes quickly enlarges channels situated at the ice-bedrock interface by the release of potential energy to the ice (Bjornsson, 1998; Huss et al., 2007). Thus, the lake drainages can actively and efficiently develop the melt water flow paths within the glacier.

2763

Furthermore, the results from the southern injection point (I2) fit well with the initial hypothesis. In both karstic springs, the Loquesse spring in the southwest and the Siebenbrunnen spring in the north, a tracer load of about one fifth of the injected tracer amount was recorded. More surprising is the absence of recovery of eosine and uranine in the Loquesse spring. Water from these two points appears to have been completely drained by sub glacial flow and Trübbach, which is rather unexpected from the model as well as from the assessments of Wildberger (1979). Both tracers were found in Siebenbrunnen spring, but this can be related to infiltration of the Trübbach downstream of the glacier rather than to infiltration directly below the glacier. However, the location of the infiltrating sections in the streambed is located south from the top of the anticline in the karst model. It can thus be expected that the upstream part of the northern syncline is drained through faults towards the Bernese springs. Accordingly, it can be argued that the bulk of the glacier melt is drained at the rock-glacier interface towards the north.

The two supplementary tracer experiments performed in 2012 reveal that the flow paths in the glacier are highly dynamic and evolve during the melting season (Covington et al., 2012). The tracer experiment performed in August 2012, just after the complete disappearance of snow on the glacier surface, revealed that at the beginning of the ice melt season the melt water also infiltrates into the karst, as tracer was found within one day in both karst springs SB and L. This was also the case in 2011 when the melt season had been ongoing for several weeks. Accordingly, it can be assumed that at the beginning of the melt season melt water infiltration into the karst is enhanced because channel in the glacier may not be well developed or compressed from the preceding winter season. With ongoing melt season the glacier channels become well developed, gradually leading over to the flow paths observed during the 2011 tracer experiment. Furthermore, the tracer experiment in August 2012 also revealed that the water table was sufficiently high from the preceding snow melt period to allow an evacuation of water towards the northern surface runoff (Fig. 11a).

2764

The last tracer experiment performed in September 2012 was conducted after a cold front lasting for several days covered the entire region with several cm of snow (up to 40 cm snow on the glacier) and stopped ice melting completely. As during this tracer experiment absolutely no tracer was detected in the surface runoff on the northern side of the glacier, it can be assumed that during these cold meteorological conditions

glacial water pressure was low due to a lack of water supply. Thus, melt water was trapped in the depression of the glacier basin and forced into the karst system which was primarily drained to the Loquesse spring close to Lac de Tseuzier (Fig. 11b). The results of the tracer experiment indicate that flow under the glacier takes place in continuous channels and that during intense snow and glacier melt the depressions are overwhelmed by a high hydrological pressure. The increase of glacial water pressure and the generated high flow velocities of melt water at the glacier bottom explain why the proportion of infiltration into the karst is reduced at high water flow conditions, compared to the expected situation at lower water input into the system. However, it is expected that the channels at the glacier bottom are changing every year and find their way through the reformed ice and on a very hard loess bed. This means that the amount of water penetrating the underlying karst can be variable; i.e. higher at the beginning of the melting season because flow could be partly pressurized and lower when pressure at the glacier bottom becomes lower.

In summary, the results of the study indicate that during melt season ice melt water of the Plaine Morte drains primarily towards Trübbach and subsequently to the Simme. Only the southernmost part of the glacier seems to clearly belong to the catchment area of the Loquesse spring, however with an overflow towards Trübbach and Simme. During low flow season the water table in the glacier basin drops, preventing an overflow towards Trübbach. In this case the southern part of the glacier is only drained to the southwestern Loquesse spring.

2765

5.2 Implications of the findings for future water resources

The simulation of melt water runoff from the Plaine Morte indicates a highly dynamic water runoff generation in the catchment. The climate change scenarios project an increase of annual and summer runoff until the mid of the century and then a drastic decrease of net runoff until the end of the century. This is an important conclusion for the water management in the future. Rapid glacier melting during the last years has favored the formation of several marginal glacier lakes around Glacier de la Plaine Morte. The sudden drainage of these lakes represents a serious hazard potential for downstream communities. With intensified ice melting the glacier lakes are expected to increase in volume over the next decades, thus potentially leading to larger floods. So far, impacts of glacier-dammed lake drainages have only been observed on the Bernese side, indicating that during outburst events water flow through the karstic system is not enhanced and flood water is primarily evacuated through fast water flow in sub glacial channels. This is consistent with results of the tracer experiment on 22 August 2011 performed on a day with strong melt water input into the system (Fig. 9a); most of the tracer re-appeared relatively fast on the Bernese side.

The long-term projections until the end of the 21st century indicate that the glacier is expected to disappear almost completely by the end of the century (Fig. 10). If this will be the case the drainage of snow and ice melt through open channels in the glacier will not be possible anymore, making drainage of snow melt water to the northern surface runoff impossible. Accordingly, downstream water resources will be affected by the loss of glacial melt water runoff. Furthermore, it can be expected that in the absence of flow channels in the glacier melt water will primarily infiltrate into the local karst and reappear at the numerous karst springs. The tracer experiments indicate that the karst system drains large parts of infiltrating water to the Loquesse spring near Lac Tseuzier. Accordingly, it can be assumed that future melt water infiltrating into the karst system may be dominantly drained to the Loquesse spring.

2766

In the small karst springs south of Glacier de la Plaine Morte no fluorescent tracer was found, indicating that water from the injection point is not drained to those karst springs. Nevertheless, the isotopic signal of the water in these karst springs indicate that during August and September these small karst springs seem to be dominantly fed with glacier melt water (Fig. 8). An absence of glacier melt water in these springs could have severe consequences for communities and ecosystems depending on spring water during the summer. Based on the presented results it is, however, still difficult to quantify the effects of climate change on water resources for these karst springs.

6 Conclusions

A combination of natural and fluorescent tracer investigations, karst modeling, glacier melt modeling and climate change projections were performed in order to identify current and future pathways of glacier and snow melt water through the karst below the Glacier de la Plaine Morte in the Bernese Oberland. The results of the tracer experiments and modeling tasks were synthesized in a thorough discussion to give an overview of current and future water resources in the downstream areas of the Plaine Morte. Based on the presented results and the subsequent discussion the conclusions can be summarized as follows:

1. Today most of the melt water during hot summer periods is drained through continuous channels at the bottom of Glacier de la Plaine Morte. During intense melting periods the water pressure in the glacier increases. Subsequently, melt water overcomes the topographic depressions of the glacier basin and follows the thalweg to the north into the surface runoff of the Trübbach. The continuous channels are formed throughout the summer and appear to be enlarged by glacier lake outbursts, which have repeatedly led to flood waves on the northern side of the Plaine Morte. During winter season melt water is trapped in the topographic depressions of the glacier basin and subsequently infiltrates entirely into the karst system and drained to the numerous karst springs.

2767

2. The isotopic composition in the karst springs around the glacier indicate that karst water is mainly composed of snow melt in spring, glacier melt in the second half of summer and local precipitation in fall. The fact that only in the three main karst springs fluorescent tracer was found indicates that the small karst is rather fed by gradual melting in the entire watershed, than by point runoff from surface melt of the Glacier de la Plaine Morte.

3. Climate change projections indicate that there will be an increase in glacier melt by 2030 to 2050 and a drastic decline by the end of the 21st century. These projections indicate that the observed rapid runoff during hot summer months will temporary intensify. Consequently, the risk of glacier lake outburst might increase. As most of the surface melt water from the Plaine Morte is drained towards Trübbach, the smaller karst springs will very likely not profit from this additional melt water.

4. By the end of the 21st century the size of the Plaine Morte will be drastically reduced, decreasing glacier melt to a minimum. This will affect water availability on the north side of the Plaine Morte, which profits currently from the rapid glacier melt. However, the ionic composition in the karst springs on the southern slopes of the Plaine Morte reveal that these springs are dominated by glacier melt during the second half of the summer. A reduction of glacier melt will evidently also impact water availability in the glacier fed karst springs.

5. Overall, it can be concluded that presently water availability is unsustainable high and that projected future water resources might severely impact water availability in karst springs fed by glacier water during the second half of summer. Nevertheless, as annual precipitation is not expected to decrease, water availability in the region is not expected to be reduced during the rest of the year.

Acknowledgements. The present study is part of the MontanAqua project (National Research Program NRP 61). The authors would like to thank the family Allemans, who allowed us to install measuring equipment on their private grounds and Joël Savioz and Maurice Perraudin from Li-
enne SA for sampling support and providing discharge data. Furthermore, we express our

2768

sincere thanks to the following persons who helped collecting water samples during the tracer experiments: Jóhannes Torfason, Jan Schwanbeck, Nina Köplin, Carol Hemund, Annette Bachmann, Michael Bühler, Barbara Lustenberger, Flurina Schneider, Mariano Bonriposi, Christine Homewood, Mauro Fischer, Leo Sold, Ueli Schneider, Guido Felder, Emmanuel Rey, Mazzal Stokvis, Michael Lindenmaier, Tilo Schneider, Antoine Marmy, Nicole Glaus, Stefano Bergamaschi, Valentin Zuchuat, Richard Mark, Silvia Hunkeler, Dominique Kröpfli, Gilles Crettaz, Marlène Travelletti and Pascale Blanc. Manuel Nitsche and Abdallah Alaoui provided valuable comments on an earlier version of the manuscript.

References

- 10 Badoux, H.: La géologie de la Zone des cols entre la Sarine et le Hahnenmoos, Mat. pour la Carte géol Suisse, 84, 1–70, 1945.
- Bauder, A., Funk, M., and Huss, M.: Ice-volume changes of selected glaciers in the Swiss Alps since the end of the 19th century, in: *Annals of Glaciology*, vol. 46, edited by: Sharp, M., Int. Glaciological Soc., Cambridge, 145–149, 2007.
- 15 Björnsson, H.: Hydrological characteristics of the drainage system beneath a surging glacier, *Nature*, 395, 771–774, doi:10.1038/27384, 1998.
- Bonacci, O., Jukic, D., and Ljubenkov, I.: Definition of catchment area in karst: case of the rivers Krka and Krka, Croatia, *Hydrol. Sci. J. – J. Sci. Hydrol.*, 51, 682–699, doi:10.1623/hysj.51.4.682, 2006.
- 20 Bühlmann, E.: Influence of particulate matter on observed albedo reductions on Plaine Morte glacier, Swiss Alps, M.Sc. thesis, University of Bern, Bern, 97 pp., 2011.
- Butscher, C. and Huggenberger, P.: Enhanced vulnerability assessment in karst areas by combining mapping with modeling approaches, *Sci. Total Environ.*, 407, 1153–1163, doi:10.1016/j.scitotenv.2008.09.033, 2009.
- 25 Coplen, T. B.: Reporting of stable hydrogen, carbon, and oxygen isotopic abundances, *Pure Appl. Chem.*, 66, 273–276, doi:10.1351/pac199466020273, 1994.
- Covington, M. D., Banwell, A. F., Gulley, J., Saar, M. O., Willis, I., and Wicks, C. M.: Quantifying the effects of glacier conduit geometry and recharge on proglacial hydrograph form, *J. Hydrol.*, 414, 59–71, doi:10.1016/j.jhydrol.2011.10.027, 2012.

2769

- Crestin, G.: Vulnérabilité du milieu karstique de la région de Montana (Valais, Suisse), M.Sc. thesis, Centre d'Hydrogéologie de l'Université de Neuchâtel, Neuchâtel, 2001.
- Crook, D. S. and Jones, A. M.: Design principles from traditional mountain irrigation systems (Bisses) in the Valais, Switzerland, *Mt. Res. Dev.*, 19, 79–99, 1999.
- 5 Doerfliger, N., Jeannin, P. Y., and Zwahlen, F.: Water vulnerability assessment in karst environments: a new method of defining protection areas using a multi-attribute approach and GIS tools (EPIK method), *Environ. Geol.*, 39, 165–176, 1999.
- Dyurgerov, M. B. and Meier, M. F.: Twentieth century climate change: evidence from small glaciers, *P. Natl. Acad. Sci. USA*, 97, 1406–1411, doi:10.1073/pnas.97.4.1406, 2000.
- 10 Farinotti, D., Huss, M., Bauder, A., and Funk, M.: An estimate of the glacier ice volume in the Swiss Alps, *Global Planet. Change*, 68, 225–231, doi:10.1016/j.gloplacha.2009.05.004, 2009.
- Farinotti, D., Usselman, S., Huss, M., Bauder, A., and Funk, M.: Runoff evolution in the Swiss Alps: projections for selected high-alpine catchments based on ENSEMBLES scenarios, *Hydrol. Process.*, 26, 1909–1924, doi:10.1002/hyp.8276, 2012.
- 15 Finger, D., Pellicciotti, F., Konz, M., Rimkus, S., and Burlando, P.: The value of glacier mass balance, satellite snow cover images, and hourly discharge for improving the performance of a physically based distributed hydrological model, *Water Resour. Res.*, 47, W07519, doi:10.1029/2010wr009824, 2011.
- 20 Finger, D., Heinrich, G., Gobiet, A., and Bauder, A.: Projections of future water resources and their uncertainty in a glacierized catchment in the Swiss Alps and the subsequent effects on hydropower production during the 21st century, *Water Resour. Res.*, 48, W02521, doi:10.1029/2011wr010733, 2012.
- Flowers, G. E., Björnsson, H., and Palsson, F.: New insights into the subglacial and periglacial hydrology of Vatnajökull, Iceland, from a distributed physical model, *J. Glaciol.*, 49, 257–270, doi:10.3189/172756503781830827, 2003.
- 25 FOEN: Auswirkungen der Klimaänderung auf Wasserressourcen und Gewässer, Synthesericht zum Projekt “Klimaänderung und Hydrologie in der Schweiz” (CCHydro), Technical report, Federal Office for the Environment, Bern, 2012.
- 30 Frei, C.: Die Klimazukunft der Schweiz, Klimaänderung und die Schweiz 2050 – Erwartete Auswirkungen auf Umwelt, Gesellschaft und Wirtschaft, Beratendes Organ für Fragen der Klimaänderung (OcCC), <http://proclimweb.scnat.ch>, last access: March 2013, 12–16, 2007.

2770

- Gabus, J. H., Weidmann, M., Sartori, M., and Burri, M.: Sierre Notice explicative, Office fédéral de topographie swisstopo, Bern, 2008.
- Goldscheider, N., Meiman, J., Pronk, M., and Smart, C.: Tracer tests in karst hydrogeology and speleology, *Int. J. Speleol.*, 37, 27–40, 2008.
- 5 Grasso, D. A. and Jeannin, P. Y.: A global experimental system approach of karst springs' hydrographs and chemographs, *Ground Water*, 40, 608–617, doi:10.1111/j.1745-6584.2002.tb02547.x, 2002.
- Gremaud, V. and Goldscheider, N.: Geometry and drainage of a retreating glacier overlying and recharging a karst aquifer, Tsanfleuron-Sanetsch, Swiss Alps, *Acta Carsol.*, 39, 289–300, 2010.
- 10 Gremaud, V., Goldscheider, N., Savoy, L., Favre, G., and Masson, H.: Geological structure, recharge processes and underground drainage of a glacierised karst aquifer system, Tsanfleuron-Sanetsch, Swiss Alps, *Hydrogeol. J.*, 17, 1833–1848, doi:10.1007/s10040-009-0485-4, 2009.
- 15 Hählen, N.: Strubel-Gletschersee Plaine Morte, Oberingenieurkreis I, Tiefbauamt des Kantons Bern, Gemeinde Lenk, 7 pp., 2012.
- Hall, D. K., Riggs, G. A., Salomonson, V. V., DiGirolamo, N. E., and Bayr, K. J.: MODIS snow-cover products, *Remote Sens. Environ.*, 83, 181–194, doi:10.1016/s0034-4257(02)00095-0, 2002.
- 20 Hock, R.: A distributed temperature-index ice- and snowmelt model including potential direct solar radiation, *J. Glaciol.*, 45, 101–111, 1999.
- Hüsler, F.: A satellite-based snow cover climatology derived from AVHRR data over the European Alps, PhD thesis, Universität Bern, Bern, 175 pp., 2012.
- Hugentobler, A.: Identifikation von Schmelzwasserfließwegen in einem karstigen Untergrund mittels fluoreszierenden Tracern, Eine Fallstudie über den Plaine-Morte-Gletscher, M.Sc. thesis, University of Bern, Bern, 2013.
- 25 Huss, M., Bauder, A., Werder, M., Funk, M., and Hock, R.: Glacier-dammed lake outburst events of Gornersee, Switzerland, *J. Glaciol.*, 53, 189–200, doi:10.3189/172756507782202784, 2007.
- 30 Huss, M., Farinotti, D., Bauder, A., and Funk, M.: Modelling runoff from highly glacierized alpine drainage basins in a changing climate, *Hydrol. Process.*, 22, 3888–3902, doi:10.1002/hyp.7055, 2008.

2771

- Huss, M., Jouvet, G., Farinotti, D., and Bauder, A.: Future high-mountain hydrology: a new parameterization of glacier retreat, *Hydrol. Earth Syst. Sci.*, 14, 815–829, doi:10.5194/hess-14-815-2010, 2010.
- Jansson, P., Hock, R., and Schneider, T.: The concept of glacier storage: a review, *J. Hydrol.*, 282, 116–129, doi:10.1016/s0022-1694(03)00258-0, 2003.
- 5 Jeannin, P., Eichenberger, U., Sinreich, M., Vouillamoz, J., Malard, A., and Weber, E.: KARSYS: a pragmatic approach to karst hydrogeological system conceptualisation, assessment of groundwater reserves and resources in Switzerland, *Environ. Earth. Sci.*, 17, doi:10.1007/s12665-012-1983-6, in press, 2012a.
- 10 Jeannin, P., Eichenberger, U., Sinreich, M., Vouillamoz, J., Malard, A., and Weber, E.: KARSYS, a pragmatic approach to Karst hydrogeological system conceptualisation, application to the assessment of reserve and resource estimation of groundwater in Switzerland, *Environ. Geol.*, in press, 2012b.
- Jobard, S. and Dzikowski, M.: Evolution of glacial flow and drainage during the ablation season, *J. Hydrol.*, 330, 663–671, doi:10.1016/j.jhydrol.2006.04.031, 2006.
- 15 Kaser, G., Cogley, J. G., Dyurgerov, M. B., Meier, M. F., and Ohmura, A.: Mass balance of glaciers and ice caps: consensus estimates for 1961–2004, *Geophys. Res. Lett.*, 33, L19501, doi:10.1029/2006gl027511, 2006.
- Maire, R.: Les karsts haut-alpins de Platé, du Haut-Giffre et de Suisse Occidentale, *Rev. Geogr. Alp.*, 65, 403–425, 1977.
- 20 Maire, R.: Les karsts sous-glaciaires et leurs relations avec le karst profond, *Rev. Geogr. Alp.*, 66, 139–148, 1978.
- Marechal, J. C., Perrochet, P., and Tacher, L.: Long-term simulations of thermal and hydraulic characteristics in a mountain massif: the Mont Blanc case study, French and Italian Alps, *Hydrogeol. J.*, 7, 341–354, doi:10.1007/s100400050207, 1999.
- 25 Paul, F., Machguth, H., and Käb, A.: On the impact of glacier albedo under conditions of extreme glacier melt: the summer 2003 in the Alps, paper presented at EARSel eProceedings, Porto, Portugal, 4, 139–142, 2005.
- Reynard, E.: Gestion patrimoniale et intégrée des ressources en eau dans les stations touristiques de montagne, PhD thesis, Université de Lausanne, Lausanne, 509 pp., 2000.
- 30 Reynard, E. and Bonriposi, M.: Integrated water use management in dry mountains of Switzerland, the case of Crans-Montans-Sierre area, paper presented at International Scientific Conference on Sustainable Development and Ecological Footprint, Sopron, Hungary, 2012.

2772

- Röthlisberger, H.: Water pressure in intra- and subglacial channels, *J. Glaciol.*, 11, 77–203, 1972.
- Schotterer, U., Stichler, W., and Ginot, P.: The influence of post-depositional effects on ice core studies: examples from the Alps, Andes, and Altai, in: *Earth Paleoenvironments: Records Preserved in Mid- and Low-Latitude Glaciers*, edited by: DeWayne Cecil, L., Green, J., and Thompson, L., Springer, the Netherlands, 39–59, 2004.
- Schuler, T., Fischer, U. H., and Gudmundsson, G. H.: Diurnal variability of subglacial drainage conditions as revealed by tracer experiments, *J. Geophys. Res.*, 109, F02008, doi:10.1029/2003jf000082, 2004.
- SGHL: Auswirkungen der Klimaänderung auf die Wasserkraftnutzung – Synthesebericht, Schweizerische Gesellschaft für Hydrologie und Limnologie (SGHL) und Hydrologische Kommission (CHy), Bern, 28 pp., 2011.
- Siemers, J. and Dreybrodt, W.: Early development of karst aquifers on percolation networks of fractures in limestone, *Water Resour. Res.*, 34, 409–419, doi:10.1029/97wr03218, 1998.
- Smart, C. C.: Statistical evaluation of glacier boreholes as indicators of basal drainage systems, *Hydrol. Process.*, 10, 599–613, doi:10.1002/(sici)1099-1085(199604)10:4<599::aid-hyp394>3.0.co;2-8, 1996.
- Voinesco, A.: Le glacier de la Plaine-Morte: épaisseur de glace et bilan de masse, M.Sc. thesis, Université de Fribourg, Fribourg, 165 pp., 2012.
- Werder, M. A., Loye, A., and Funk, M.: Dye tracing a jokulhlaup: 1. Subglacial water transit speed and water-storage mechanism, *J. Glaciol.*, 55, 889–898, 2009.
- Wildberger, A.: Beiträge zur Karsthydrologie des Rawil-Gebietes (Helvetische Kalkhochalpen zwischen Wildhorn und Wildstrubel), Ph. D. thesis, Universität Bern, Bern, 343 pp., 1979.
- Wildberger, A., Jeannin, P., and Pulfer, T.: Hochwasser 1999 und 2000 im Hölloch (Zentralschweiz) Beobachtung und Folgen, Actes du 11 Congrès National de Spéléologie, Genève, Switzerland, 81–88, 2001.

2773

Table 1. Overview of available data and observations.

Map/information		Karstic 3-D model resolution		Source	
Geologic map		1 : 25 000		Swiss geologic survey	
15 geological cross sections		1 : 25 000/1 : 50 000		Available at ISSKA	
DEM		25 m × 25 m		Swisstopo	
Meteo and snow cover data					
Parameter	Location ^a	Sampling period	Unit	Frequency of sampling	Source
Snow Height and Temperature	W1	2011–2012	cm; °C	daily	SLF ^b
Temperature	W2	2011–2012	°C	daily	CMA ^b
Temperature, Precipitation	CM	2011–2012	°C; mm	daily	MeteoSwiss
Snow cover area ratio		2001–2012	–	daily	(Hall et al., 2002)
Tracer Experiment					
Water sampling (APEG)	GW, OR, SB, R, SB, TB, L and more ^c	22 Aug 11 –31 Aug 11	mg m ⁻³	1, 4, 6, 8, 12, 24 h	Authors/FOEN
Discharge	LT, OR, TB, SB, GW ^d	1993–2012	m ³ s ⁻¹	5 min/daily	FOEN/authors/ Lienne SA
Glacier melt modeling					
Data set	Location ^a	Sampling period	Unit	Frequency of sampling	Source
Mass balance	PM	2010/2011	mm w eq	2 per year	Authors
Digital Elevation Model	PM	1956 and 2005			Authors
Ice thickness	PM	2010	m		Authors
Climate scenarios		2010–2100			(Frei, 2007)

^a LT = Lac de Tseuzier, CM = Crans-Montana, GW = Grubenwald, OR = Oberried, SB = Siebenbrunnen, TB = Trübbach, L = Loquesse, PM = Plaine Morte, W1 = weather station operated by SLF, W2 = weather station operated by CMA.

^b SLF = Institute for Snow and Avalanche Research, Davos; CMA = Sensalpin on behalf of *Remontées mécaniques de Crans-Montana*.

^c Over 30 karst springs were sampled during tracer experiments. Locations where no tracer was detected are not named and only visualized in Fig. 1.

^d At GW and OR the FOEN operates stationary gauging stations; discharge at other locations was estimated with pressure sensors converted to continuous (5 min resolution) discharge time series with periodic discharge measurements using the salt method (Hugentobler, 2013). Daily discharge into Lac de Tseuzier is computed from reservoir level and drainage by Lienne SA.

2774

Table 2. Overview of the tracer injections.

Date and time ^{a,b}	Tracer	Amount	Location of injection ^a
22 Aug 2011, 13:30 (S2)	Eosine	36 kg	I1 (604202/137013)
22 Aug 2011, 12:45 (S2)	Duasyne	38.4 kg	I2 (604871/136339)
22 Aug 2011, 11:40 (S2)	Uranine	12 kg	I3 (607002/136471)
6 Aug 2012, 11:05 (S1)	Uranine	8 kg	I2 (604262/136376)
2 Sep 2012, 11:00 (S3)	Uranine	4 kg	I2 (604262/136376)

^a Locations are given in Swiss grid system CH1903 and visualized in Fig. 1.

^b S1, S2 and S3 represent typical situations during summer season as outlined in the discussion section.

2775

Table 3. Overview of amount of tracer found in karst and surface runoffs after the injections in August 2011.

Location	Abrev.		Duasyne [kg]	Uranine [kg]	Eosine [kg]
Total injected amount			38.4	12	36
Location (type)		Canton	Amount of tracer found at locations		
Oberried (surface)	OR	BE	12.5	8	36.7
Grubenwald (surface)	GW	BE	8.4	9.5	41.9
Retzliberg (karst)	R	BE	traces	traces	traces
Siebenbrunnen (karst)	SB	BE	traces	traces	traces
Loquesse (karst)	L	VS	9.3 ± 0.1*	nothing	nothing
Mean flow velocity [km h ⁻¹]					
Trübbach (surface)	TB	BE	2.4	3.0	–
Oberried (surface)	OR	BE	3.8	3.9	2.7
Grubenwald (surface)	GW	BE	6.7	7.4	6.0
Siebenbrunnen (Karst)	SB	BE	0.1	0.2	0.2
Retzliberg (Karst)	R	BE	–	0.5	0.4
Loquesse (Karst)	L	VS	0.4	–	–

* Uncertainty was estimated with six different integration methods to compute loading as described in Hugentobler (2013).

2776

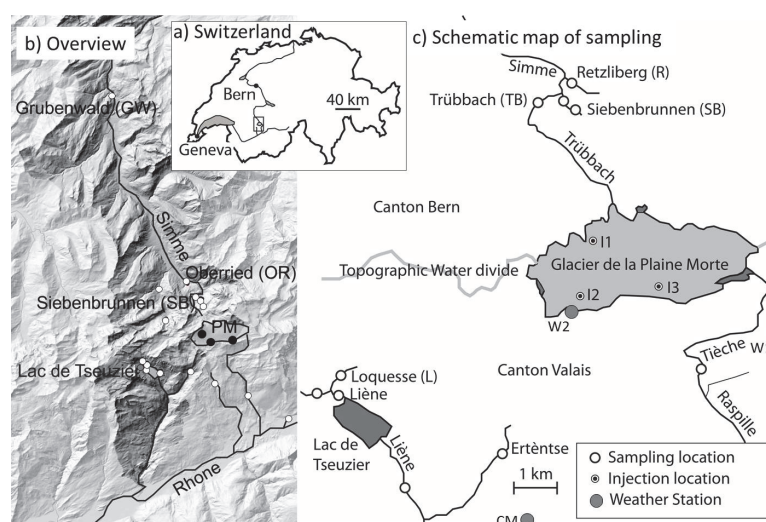
Table 4. Overview of the temporal evolution of the amount of tracer found in karst and surface runoffs.

Location	Abrev.	Duasyne	Uranine	Uranine	
Injection date		22 Aug 2011 (S2)	6 Aug 2012 (S1)	2 Sep 2012 (S3)	
Mean T at M2 [°C]		12.5	8.5	0.4	
Snow Height at M1 [cm]		0	0	~ 30 ^a	
Ratio of Snow cover Area		0	0.03	0.15	
Total injected amount [kg]		38.4	8	4	
Location (type)		Canton	Amount of tracer found at locations [kg] ^b		
Oberried (surface)	OR	BE	12 kg	1.0	–
Grubenwald (surface)	GW	BE	8.8 kg	1.3	–
Retzliberg (karst)	R	BE	traces	–	–
Siebenbrunnen (karst)	SB	BE	traces	0.01 ± 0.001	–
Trübbach (surface)	TB	BE	n.s.	0.5 ± 0.1	–
Loquesse (karst)	L	VS	12 kg	4.5 ± 0.2	4.4 ± 0.3
Mean flow velocity [km h ^{−1}]					
Trübbach (surface)	TB	BE	2.3	1.6	–
Oberried (surface)	OR	BE	3.8	3.4	–
Grubenwald (surface)	GW	BE	6.6	3.8	–
Siebenbrunnen (Karst)	SB	BE	0.1	0.2	–
Loquesse (Karst)	L	VS	0.3	0.5	0.2

^a On 2 Sep a snow height of ~ 30 cm was recorded; however measurements close to the injection point I2 revealed ~ 40 cm of snow heights.

^b Uncertainties were estimated with six different integration methods to compute loading as described in Hugentobler (2013).

2777

**Fig. 1.** Overview of the study site including the surroundings of the Glacier de la Plaine Morte (PM). **(a)** locates the study area with a square in Switzerland, **(b)** gives a topographic overview of the two valleys to the north and south of the PM (darkened area delimits topographic watershed of the Simme and the Liène) and **(c)** illustrates schematically sampling locations around PM. Dark grey areas on the border of PM illustrate temporary glacier lakes.

2778

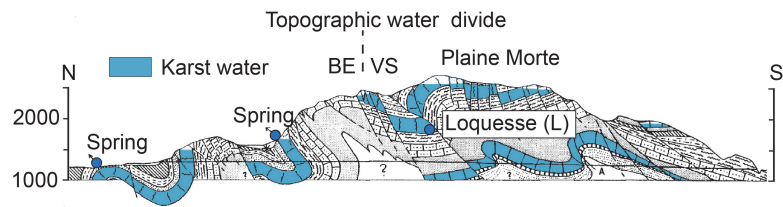


Fig. 2. Geological cross-section along Oberried, Siebenbrunnen and Lac de Tseuzier. Urgonian Limestone and Malm limestone karstic aquifers are highlighted in blue. The Loquesse spring (L) is projected according to geology. Modified after Wildberger (1979).

2779

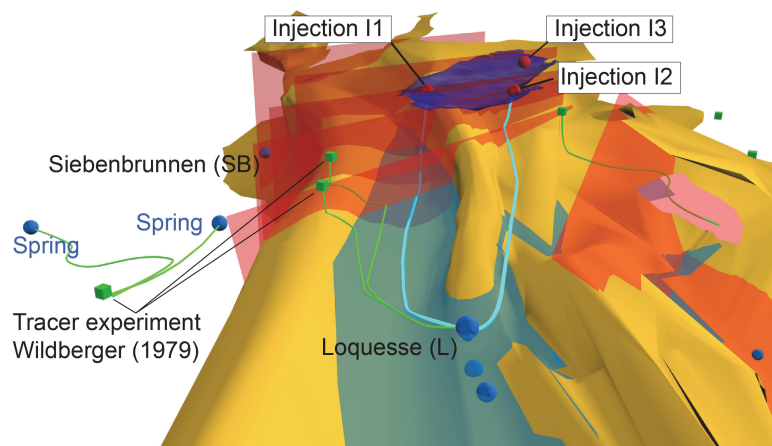


Fig. 3. 3-D view towards the East of the Urgonian limestone basis (top of Valanginian Marls). Red and transparent planes are faults. Tracing experiments previously carried out are represented in green, including the expected underground flow paths. The Plaine Morte is visible in the middle (dark blue). Blue spheres are karstic springs. The blue surfaces with some transparency are karstic nappes.

2780

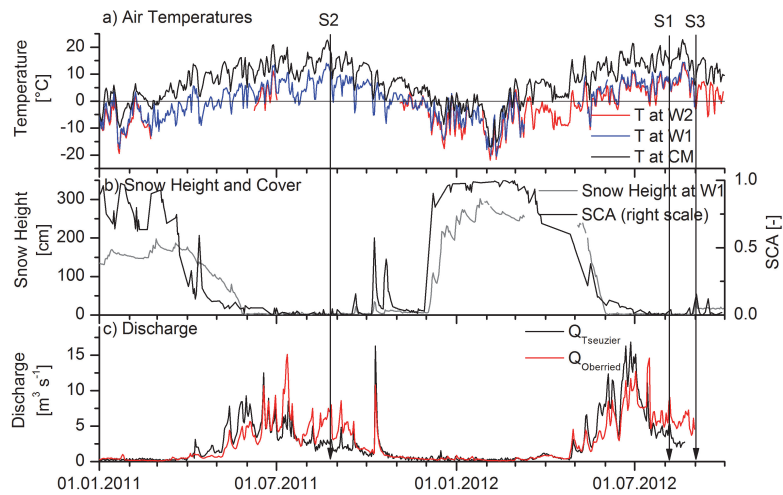


Fig. 4. Hydro-meteorological observations in the region of the Glacier de la Plaine Morte: **(a)** illustrates mean daily air temperatures at W1, W2 and CM, **(b)** shows the snow height at W1 and the ratio of snow cover area (SCA) in the entire watershed depicted in Fig. 1 and **(c)** displays mean daily total discharge into Lac de Tseuzier ($Q_{Tseuzier}$) and at Oberried ($Q_{Oberried}$). S1, S2 and S3 illustrate tracer injection dates.

2781

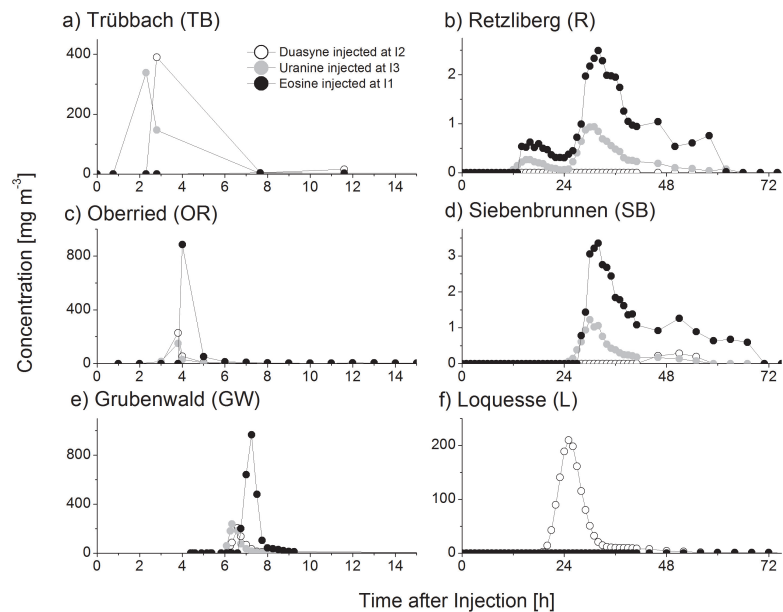


Fig. 5. Temporal evolution of tracer concentration after simultaneous tracer injection at locations I1, I2 and I3 (see Fig. 1) on Glacier de la Plaine Morte in August 2011.

2782

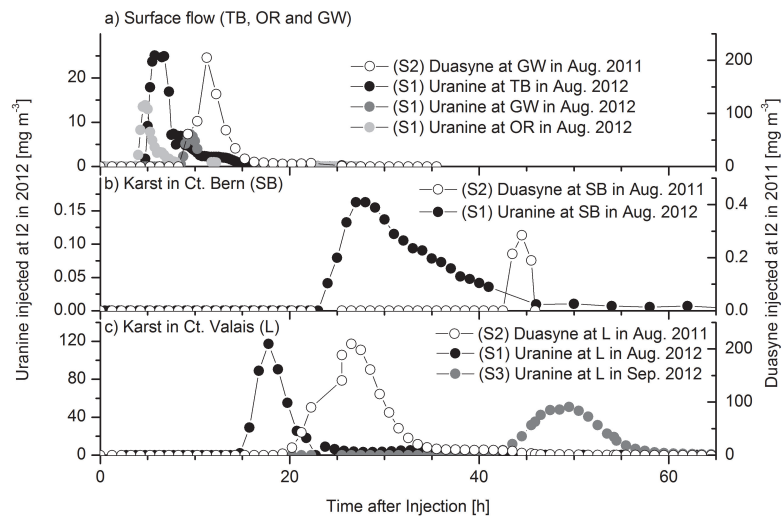


Fig. 6. Temporal evolution of tracer concentration after injection at the southern location (I2). **(a)** Concentrations in surface runoff at TB, OR and GW, **(b)** concentrations in karstic spring SB on the northern side of the glacier and **(c)** concentrations in karstic spring L on the southern side of the glacier.

2783

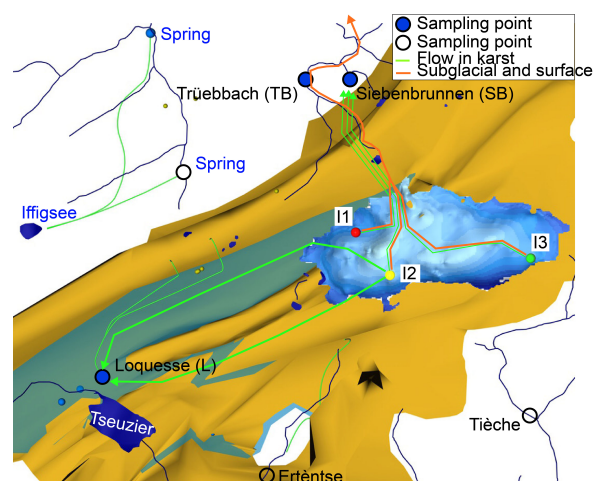


Fig. 7. Visualization of the karst system assembling all data in the karst model.

2784

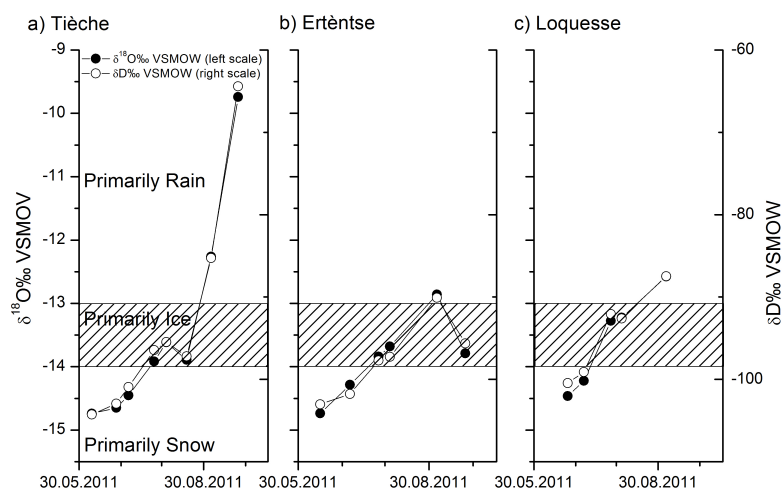


Fig. 8. Temporal development of isotopic composition at selected karst springs south of the Plaine Morte. Typical isotopic signatures found in snow samples are illustrated with striped area. Locations are shown in Fig. 1.

2785

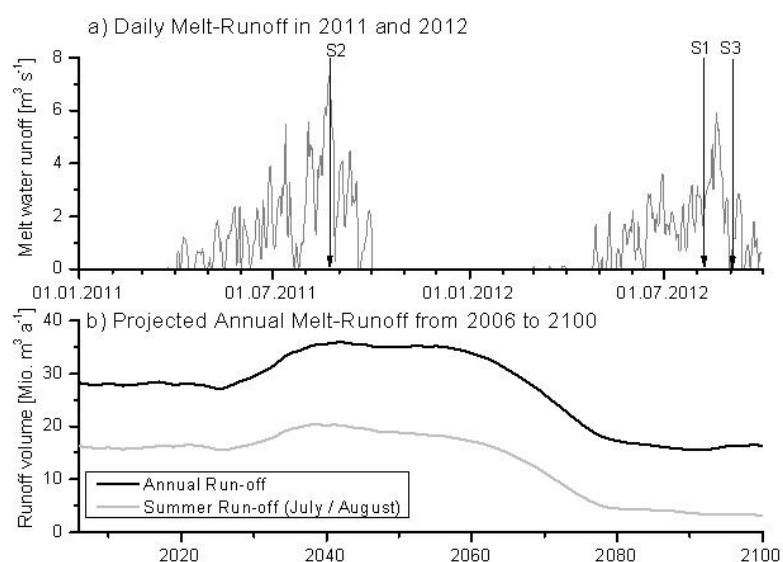


Fig. 9. (a) Calculated melt water runoff from the surface of the Plaine Morte in 2011 and 2012. The three dates of the tracer injections are illustrated in the figure with an arrow labeled with the according situation. **(b)** 20-yr running means (annual runoff and the summer runoff) of projected future runoff volume from the basin of the Plaine Morte driven with a median climate change scenario.

2786

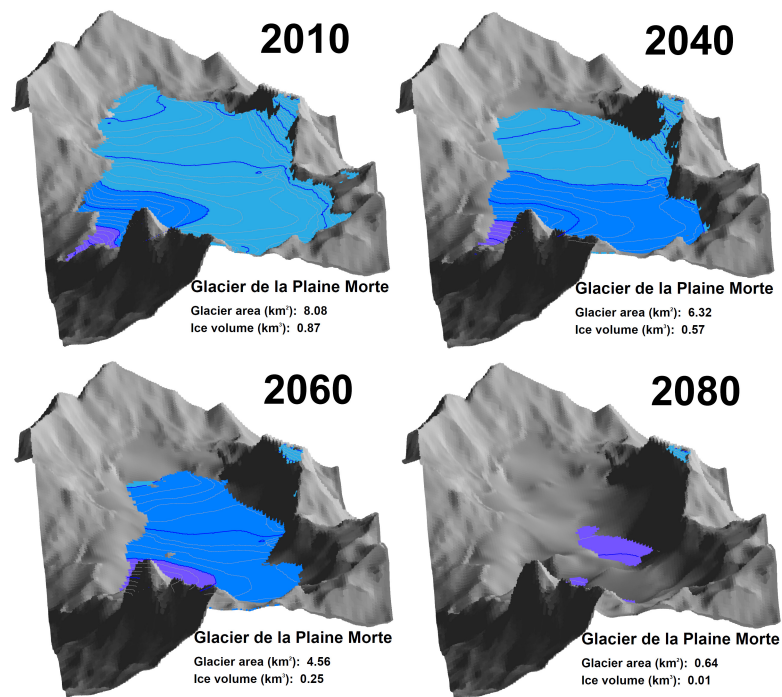


Fig. 10. Modeled future retreat of the Plaine Morte in 2010, 2040, 2060, and 2080. Colors indicate surface elevation bands of the glacier. The glacier area and volume for each time slice is given.

2787

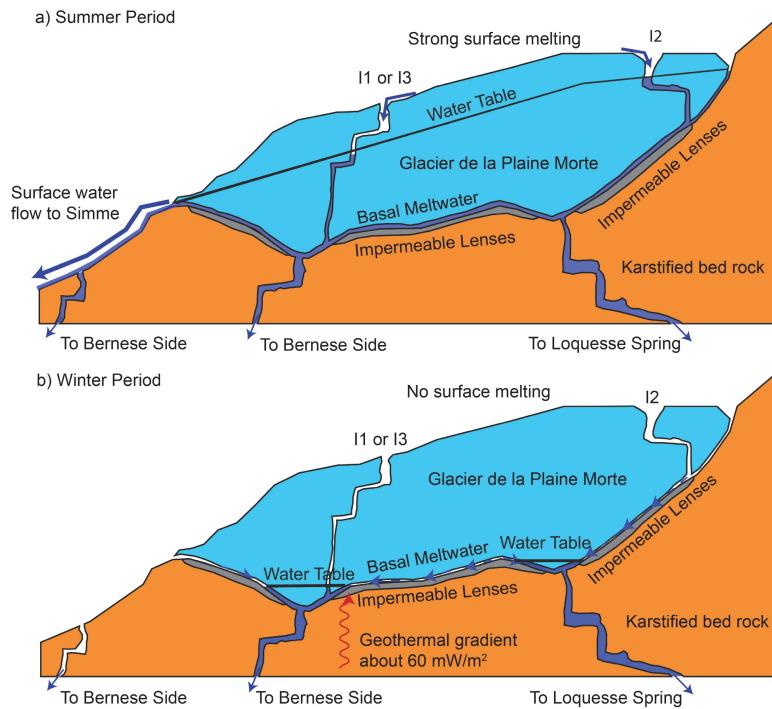


Fig. 11. Schematic sequence of drainage of melt water in sub glacial, karstic and surface flow paths during **(a)** summer season and **(b)** winter season.

2788